ESA STUDY CONTRACT REPORT

No ESA Study Contract Report will be accepted unless this sheet is inserted at the beginning of each volume of the Report.

ESA Contract No: 4000122018/17/NL/PS/gp	SUBJECT: Test of LVF based algorithms on a compact hyperspectral imager (COSI)	CONTRACTOR: Vlaamse Instelling voor Technologisch Onderzoek NV (VITO)
ESA CR(No): 4000122018/17/NL/PS/gp	No. of Volumes: 1 This is Volume No: 1	CONTRACTOR'S REFERENCE: COSI 1710641 D4

ABSTRACT

This document contains an executive summary of the outputs of the COSI project. It summarizes in brief the findings and achievements within the project..

The work described in this report was done under ESA Contract. Responsibility for the contents resides in the author or organisation that prepared it.

Names of authors:

S. Livens, B. Delauré

NAME OF ESA STUDY MANAGER:

Alessandro Zuccaro Marchi

DIV: TEC-MMO

DIRECTORATE: D/TEC

D4 COSI Executive Summary

Status information

Security classification:	Non confidential	State:	Final
Current version number:	1.1	Date of first issue:	28/06/2019
Prepared by:	S. Livens	Date:	05/07/2019
Verified by:	B. Delauré	Date:	05/07/2019
Approved by:	B. Delauré	Date:	05/07/2019

Copyright notice

1. PROJECT OBJECTIVES AND WORK LOGIC

The **project objectives** are summarized as follows:

- development of an automated processing system running on a standalone processing machine for a linear variable filter based compact hyperspectral camera
- validation of the algorithmic processing approach and the image product quality based on drone based data acquisitions
- demonstration of the system

2. COSI SYSTEM DESIGN

The COSI system compact hyperspectral camera system consists of 2 subsystems: the hardware was defined and fixed, while the software system was developed, specifically for processing image acquisitions from the camera.

2.1 Hardware: Camera Specification

The hardware chosen within the project is a compact hyperspectral camera system suitable for deployment on a small drone. We used the Cubert ButterflEYE LS S199 camera (see Figure 1), which is based on a CMOSIS CMV2000 CMOS sensor chip, equipped with directly deposited narrow-band interference filters.

Figure 1 photo of the Cubert ButterflEYE-LS S199 compact hyperspectral camera

2.2 Software: processing solution development

We designed an automated processing system based on existing prototype processing modules, which were reimplemented for greater efficiency and user friendliness. The objective was to develop a stand alone processing solution which entirely runs on the user side.

All necessary input data from a data acquisition campaign is collected using the GUI (Graphical User Interface). Minimum required inputs are: raw imagery, GPS information for each single image and camera calibration information (geometric, radiometric and spectral)

Next the user is able to configure his desired hyperspectral workflow and required output products. Besides the standard output products, the GUI will support the input of raster calculations for creating custom vegetation index maps.

Once the configuration is set, the user is able to start the automated hyperspectral processing workflow. This hyperspectral processing workflow can be split into a couple of modules, each of which consists of multiple tools which are ported to uniform programming languages (Java and Python) and a limited set of 3rd party libraries.

The processing workflow consists of the following main blocks:

- Geometric Processing
- Projection & Data reshaping:
- Radiometric Processing
- Raster Processing

The COSI Software transforms the raw image data of the COSI camera into the image products: Digital Surface Model (DSM), Hyperspectral Data Cube, True color composite and False color composite. Additionally the Data Quality component verify the quality of the input and output data and reports this to the user in a automatically generated quality report.

The final version of the COSI software contains several CPU and GPU routines to optimize for speed. Also the amount of operator interventions and operator time needed were strongly reduced. Both measures resulted in a significant decrease of the processing time: from 19 hours to 77 minutes for a reference dataset.

3. SYSTEM AND CAMERA TEST

The purpose of the tests is to validate the camera requirements and to execute functional camera tests to ensure a smooth camera usage during calibration activities and data acquisitions missions.

The **first phase of the tests** focused on the mechanical and functional testing of the camera as stand-alone component, already validating most of the requirements and preparing the camera for the lab test and calibration. All foreseen tests were carried out with good result..

The **second phase** focuses on the calibration and validation of the requirements which required specialized lab equipment. The characterisation by manufacturer describes the combined characteristics of sensor and of the filters. However we established a characterization of the complete camera system, including the optics, which is very important for achieving good spectral and radiometric quality.

We performed detailed measurements of the Dark current and Pixel Response Non Uniformity (PRNU), the latter using three different techniques (in the lab and outdoors). Both measurements are essential inputs to the processing as they are needed to convert raw data radiometrically.

The bulk of the efforts were spent on spectral measurement using a test environment with an integrating sphere and monochromator. In automated tests spectral sweeps were carried out with a monochromator over the whole wavelength range and repeated for different integration times. To ensure good characterization of the out-of-band spectral transmission, which only yields very weak signal, additional sweeps with a wider peak (5 nm instead of 1 nm) were also carried out. Together this resulted in a very detailed spectral characterization of the sensor.

The **third phase** handles the RPAS related topics. In this phase the camera is mounted on the RPAS and tests are executed with the operating equipment. Some tests will require an environment with GPS coverage. This phase also includes a test flight on a test field, to fly and operate the camera. At the end of this phase, the camera is integrated on the RPAS and ready to fly the first mission.

The **fourth and last phase** is a mission execution and interface test towards the processing chain. It makes use of the field software to perform input data checks on the raw data and to upload the data towards the processing chain. .

4. VALIDATION

The system validation and image quality assessment, testing both the camera system and the processing solution, has been carried out in three themes:

- validation of radiometric performance (using artificial targets)
- validation of geometric performance (using artificial targets)
- validation of application missions. (using relevant agricultural scenes)

The first two themes make use of a dedicated validation mission. This mission has been executed over a grass field on which artificial targets were deployed. Its goal was to provide data for both geometric and radiometric validation under semi-controlled conditions, a view of the layout of the targets is shown in Figure 2 The application missions were executed over crop fields where variability is either induced in an experimental field setup (controlled application mission) or is naturally present along with some control plots on a production field (semi-controlled application). There were multiple mission over time. They also serve as input to the temporal radiometric validation.

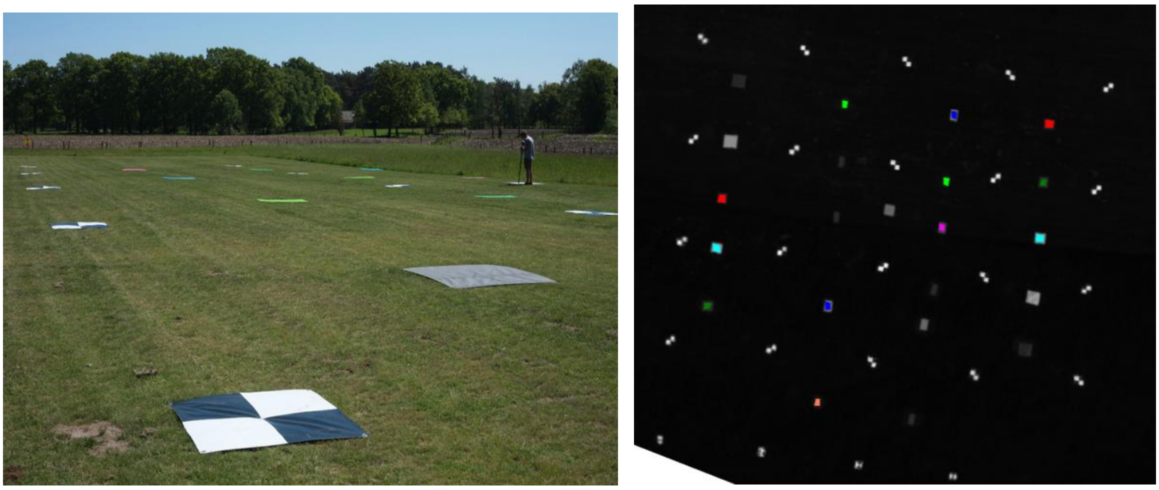

Figure 2: left: field with targets laid out for the validation flight, right: hyperspectral image product showing targets on field

4.1 Radiometric Validation

The radiometric validation consists of 4 distinct parts, an overview of results is given in Table 1

Table 1: Overview of radiometric validation results

	COSI		MicroHyperspec		ASD	
	RMS	SA	RMS	SA	RMS	SA
absolute	0.019	2.26	0.023	1.12	0.028	1.32
spatial	0.012	1.27	0.012	1.07	0.023	0.44
per pixel	0.016		0.012		0.012	
temporal	0.019	2.87				

Absolute Correspondence: To quantify how well spectra from the COSI system correspond to known reference, we collected average spectra over reference targets and compared them to the manufacturers reference. The results show that the COSI system yields small absolute RMS errors, smaller than the MicroHyperspec alternative hyperspectral imager. The spectral angle differences also well under control, but they are comparatively upto 2x larger, indicating some minor artefacts in the shape of the spectra.

Spatial Consistency over the field of view was investigated by comparing average spectra of identical targets laid out over the field. The absolute RMS errors are very small, smaller than the absolute errors. The spectral angle differences are again somewhat larger for the COSI system, but remain small.

Pixel to Pixel variability was investigated by comparing the single pixels spectra within a target to target average spectra. The COSI results are very good, with RMS errors are smaller than the absolute errors, and also smaller than those of the MicroHyperspec, which exhibits increased noise in the NIR region.

Temporal consistency was verified by comparing the spectra from identical targets in acquisitions at different points in time. The absolute errors vary over time, but stay in the same range, with an average similar to the estimated absolute errors.

We conclude that the COSI system can produce competitive radiometric quality compared to the MicroHyperspec system.

4.2 Geometric Validation

The goal of the geometric validation was to evaluate the performance of the processing chain and the quality of the end products in terms of relative and absolute geometric accuracy of the entire hypercube, and band alignment accuracy within the hypercube. This was done by quantifying residual errors on photo-identifiable points in the field in all dimensions.

Results of two processing scenarios have been investigated: with or without the use of GCPs, summary numbers are given in Table 2.

As expected, absolute errors are very large without GCPs. With GCPs, an unknown bug causes them to be still too high. Relative erros are obtained by correcting for the overall shift, resulting relative errors are much smaller, esp. when GCPs have been used. Most imporntant is however the coregistration errors measured locally on the features. In both processing scenarios, the coregistration errors are below 5cm, thus below 1 GSD. This demonstrates that overall band alignment accuracy is within 1 pixel for a hypercube GSD of 0.05 m. The use of GCPs It is not necessary to use GCPs to achieve this accuracy, these are only needed to achieve the highest possible relative and absolute accuracy (e.g. for pixel-level multitemporal studies).

Table 2: overview of geometric validation results

error in [m]	X	Y	Z	combined
without GCPs				
absolute error	-8.740	-2.608	-2.533	**9.466**
relative error	0.204	0.342	0.150	**0.426**
coregistration	0.030	0.025		**0.039**
with GCPs				
absolute error	1.014	0.126		**1.022**
relative error	0.038	0.026	0.060	**0.076**
coregistration	0.038	0.029		**0.048**

4.3 Validation of Application Missions

The aim of the application mission is to assess the hypercube reflectance values on crop types relevant for hyperspectral remote sensing analysis in quantifying and identifying several types of stress.

Semi-controlled potato production

The potato field consisted of a normally treated production field on which 3 experimental treatment zones were delineated, with the intent to investigate to what extent remote sensing can be used to discern water stress from nutrient stress and to provide appropriate management advise. From the resulting spectra, we could not find no significant differences between fertilization treatment zones. This was most probably due to the extended drought period. Only the non-irrigated treatment zone could be discerned statistically

Controlled application with grass fertilization.
The trial field consisted of 4 x 8 zones (each measuring 12 x 6 m) receiving different doses of mineral nitrogen and potassium through different types of fertilized. The goal of the study was to evaluate the effects of yield and quality of the grass at each harvest to serve as cattle feed. For each treatment zone, the yield was measured from the harvest, and statistics were calculated for each index map produced by the COSI software. The calculated vegetation indices did not seem to correlate intuitively with the yield measurements. By comparing the index maps to the DSM (also generated by the COSI processing software), we able to find the root cause. For the zones with highest yield, the grass elevation was lower due to lodging. Lodged grass has different spectral properties, causing lower vegetation index values.

5. Conclusion

Overall we have demonstrated the capabilities of the COSI hyperspectral imaging system. The overall excellent band coregistration results are reassuring: they demonstrate that the COSI system, in which the spectral bands of a single point are not acquired simultaneously, can also produce reliable spectra at pixel level. This is affirmed by the radiometric evaluation where the accuracy of the results is in most aspects competitive with established hyperspectral imagers.

Also the processing duration has been significantly reduced from 19 hours to 77 minutes for a reference dataset. This has been achieved by minimizing operator intervention and optimizing routines for GPU and CPU execution.

The application missions demonstrate that the quality of the results makes them perfectly usable for applications studies. We especially mention the advantage of the COSI system: the additional DSM product produced by default allowed to understand the lodging phenomenon, which would not be possible for hyperspectral data alone.